AD-A103 807 FULMER RESEARCH INST LTD STOKE POGES (ENGLAND) F/G 11/6
CHARACTERIZATION OF URANIUM-3/4% TITANIUM ALLOYS EXTRUDED FROM --ETC(U)
JUN 81 R I SAUNDERSON, G B BROOK DAJA37-79-C-0100
UNCLASSIFIED R812/4 NL

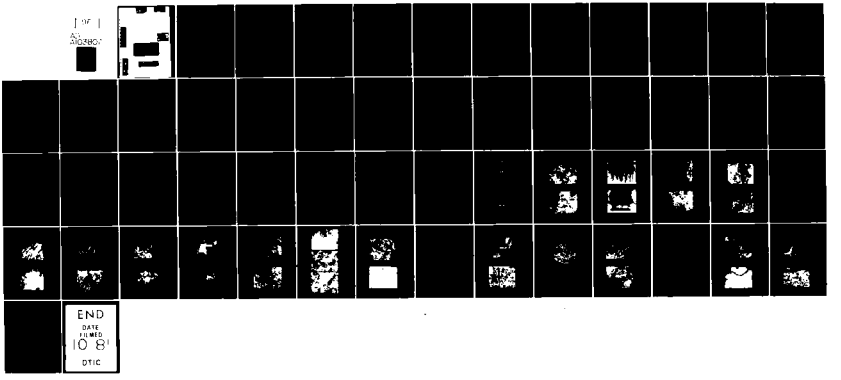

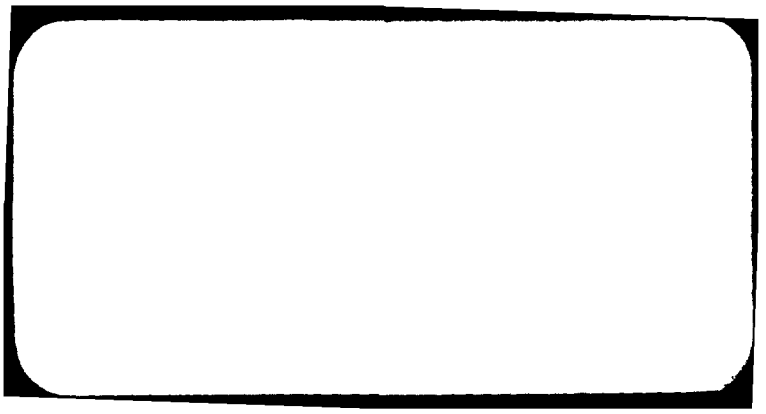

(4)

CHARACTERISATION OF URANIUM-¾ % TITANIUM ALLOYS EXTRUDED FROM THE GAMMA PHASE.

FINAL REPORT,

by

R.I. Saunderson and G.B. Brook

R812/4/June 1981

Contract Number DAJA 37-79-C-0100 R&D 2622

144400

UNCLASSIFIED

SECURITY CLASSIFICATION OF THIS PAGE (When Data Entered)

R&D 2622-MS

REPORT DOCUMENTATION PAGE	READ INSTRUCTIONS BEFORE COMPLETING FORM
1. REPORT NUMBER / 2. GOVT ACCESSION NO. AD-A103 807	3. RECIPIENT'S CATALOG NUMBER
4. TITLE (and Subtitle) Characterisation of Uranium- % Titanium Alloys Extruded from the Gamma Phase	5. TYPE OF REPORT & PERIOD COVERED Final Technical Report
	6. PERFORMING ORG. REPORT NUMBER
7. AUTHOR(s) R. I. Saunderson and G. B. Brook	8. CONTRACT OR GRANT NUMBER(s) DAJA37-79-C-0100
9. PERFORMING ORGANIZATION NAME AND ADDRESS Fulmer Research Institute Limited Stoke Poges Slough, UK	10. PROGRAM ELEMENT, PROJECT, TASK AREA & WORK UNIT NUMBERS IT161102BH57-04
11. CONTROLLING OFFICE NAME AND ADDRESS USARDSG-UK Box 65 FPO NY 09510	12. REPORT DATE June 1981
	13. NUMBER OF PAGES 42
14. MONITORING AGENCY NAME & ADDRESS (if different from Controlling Office)	15. SECURITY CLASS. (of this report) Unclassified
	15a. DECLASSIFICATION/DOWNGRADING SCHEDULE

16. DISTRIBUTION STATEMENT (of this Report)

Approved for Public Release - Distribution Unlimited

17. DISTRIBUTION STATEMENT (of the abstract entered in Block 20, if different from Report)

18. SUPPLEMENTARY NOTES

19. KEY WORDS (Continue on reverse side if necessary and identify by block number)

Extrusion, quench rate, ageing, centerline cracking, void formation, texturing, preferred orientation, hardness, microstructure

20. ABSTRACT (Continue on reverse side if necessary and identify by block number)

The effects of quench rate, mode of quenching and subsequent ageing treatments on microstructure and properties of a U- wt % Ti alloy have been investigated. Particular emphasis has been placed upon heat treatment of 35mm diameter, γ -extruded, bar. Cooling rates in the range 2 - 480 ks^{-1} were obtained, resulting in a wide spectrum of microstructures ranging from granular α after slow rates of cooling to almost fully martensitic α' after faster cooling. By optimising

DD FORM 1 JAN 73 1473 EDITION OF 1 NOV 65 IS OBSOLETE

UNCLASSIFIED

SECURITY CLASSIFICATION OF THIS PAGE (When Data Entered)

Continued ...

20. the rate and mode of quenching the problems of centreline cracking and void formation have been circumvented. Subsequent ageing at 450°C produced hardnesses in excess of 480 Hv_{30} due to precipitation of U_2Ti.

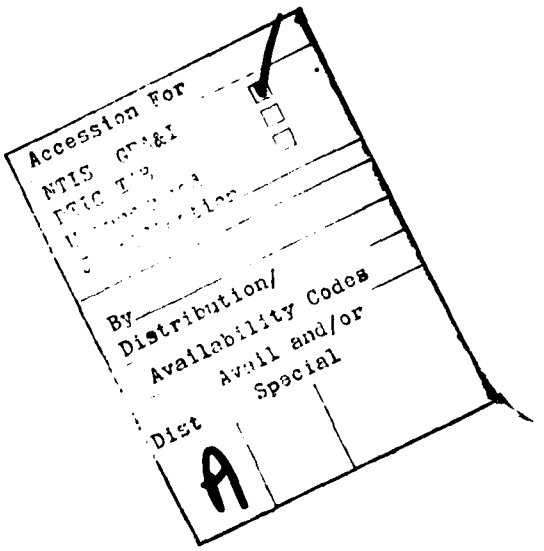

FULMER RESEARCH LABORATORIES LIMITED

CHARACTERISATION OF URANIUM-¾ % TITANIUM ALLOYS EXTRUDED FROM THE GAMMA PHASE

FINAL REPORT

by

R.I. Saunderson and G.B. Brook

R812/4/June 1981

Contract Number DAJA 37-79-C-0100 R&D 2622

SUMMARY

High density and tensile properties can be achieved in U-¾ % Ti by water quenching from the γ phase and subsequently ageing at lower temperature. These high quench rates have been found to give rise to centreline cracking and void formation in medium and large diameter bars (i.e. greater than approximately 20mm diameter).

In the present work the effects of quench rate, mode of quenching and subsequent ageing treatments on microstructure and properties of a U-¾ wt % Ti alloy have been investigated. Particular emphasis has been placed upon heat treatment of 35mm diameter, γ-extruded, bar.

Cooling rates in the range 2 - 480 Ks^{-1} were obtained, resulting in a wide spectrum of microstructures ranging from granular α after slow rates of cooling to almost fully martensitic α' after faster cooling. By optimising the rate and mode of quenching the problems of centreline cracking and void formation have been circumvented.

Even at the fastest cooling rates only approximately half to three-quarters of the available titanium was retained in solution. Nevertheless, subsequent ageing at 450°C produced hardnesses in excess of 480 Hv_{30} due to precipitation of U_2Ti.

Extrusion in the γ phase resulted in a pronounced texture with (002) perpendicular to the extrusion direction. This preferred

orientation could be eliminated or diminished by reheating into the γ phase. Pronounced texturing was not produced in bars by controlled immersion. However, other work on α-extruded bars has shown that it is possible to induce prominent textures by this method.

CONTENTS

1. INTRODUCTION

Alloys of uranium with molybdenum or titanium have been developed as possible penetrator materials because of their high hardness and tensile strength[1]. Of the titanium containing alloys the composition U-¾% Ti has been selected for further investigation. The alloy is produced commercially by casting into 8" and 12" diameter ingots and subsequently extruding in the γ phase to 1¾" diameter rod. To obtain optimum properties the extruded rod must be quenched from the γ phase and aged to peak hardness at temperatures in the region of 400 - 500°C. Moderately high quench rates are required to retain sufficient titanium in solution to give a satisfactory age hardening response. At these quench rates non-uniform microstructures across the section of bars greater than approximately ¾" diameter give rise to problems of centreline cracking and void formation.

The aim of the present work has been to obtain a better understanding of the effects of post extrusion thermal treatment on the microstructure and properties of a U-¾wt % Ti alloy. Particular emphasis has been placed upon the effect of various modes of quenching and the subsequent ageing of full sized bar specimens, 35mm in diameter. The possibilities of inducing a transformation texture in these bars by controlled immersion quenching have also been investigated.

2. TECHNICAL BACKGROUND

i) The Equilibrium Phase Diagram

The uranium-titanium phase diagram has been studied by several workers[2,3,4]. The most comprehensive work is that due to Knapton[5] who reported that above 898°C, γ-uranium and β-titanium form a complete range of solid solutions. An intermediate ε-phase (U_2Ti) forms from γ-uranium at 898°C and 9.02 wt% Ti. A eutectoid reaction exists at 0.83 wt% Ti and 723°C by which γ-uranium decomposes to β-uranium and U_2Ti. The β phase transforms to $\alpha + U_2Ti$ at 667°C and the solubility of titanium in α-uranium is less than 0.18 wt% Ti. The uranium-rich region of the uranium-titanium equilibrium phase diagram due to Knapton[5] is shown in Figure 1. Similar findings have been reported by Udy and Boulger[3,4] but are at variance with Knapton's findings concerning the range of the U_2Ti field, the γ-eutectoid position and the solubility of titanium in α-and β-uranium. The results of Knapton have, however, been confirmed by several workers[6 - 8] and his interpretation of the phase diagram is now widely accepted and has been used throughout the present work.

ii) Nomenclature

The nomenclature used in the present work to denote the various metastable phases and variants was that proposed by Lehmann and Hills[9] in which the symbol α denotes structures which are modifications of orthorhombic α-uranium. A superscript denotes deviations from the orthorhombic structure. The structure resulting from a relative contraction of the 'b' lattice parameter is designated α' while that derived from a relative contraction of the 'b' parameter in conjunction with a change to a monoclinic structure is denoted by α". Morphological characteristics are denoted by subscripts. The subscripts 'a', 'b' and 'n' are used to denote acicular, banded and nucleation and growth type structures respectively. In a similar manner, superscripts are used to denote crystallographic deviations from the bcc γ-phase. For instance a tetragonal variation of γ would be designated γ^o.

3. EXPERIMENTAL DETAILS

Two quenching furnaces have been constructed and used in the present work. The first, a gas quenching furnace, was described in detail in a previous report[10] and comprised of an evacuated column in which the specimen was held and induction heated. Quenching was achieved by opening the vacuum to a reservoir of either argon or helium gas. Quench rates of up to 480 Ks^{-1} were achieved in this way.

The second furnace facilitated liquid quenching of full sized bars under vacuum. The final design is shown diagrammatically in Figure 2. The system was pumped by a 2" oil diffusion pump with liquid nitrogen cold trap. A vacuum of 3×10^{-6}mb was achieved regularly at room temperature. (The pressure was measured at the bottom of the furnace tube). Outgassing for a minimum of 12 hours at 500°C was necessary in order that the vacuum, during subsequent heating to 780°C, should not deteriorate to worse than 3×10^{-4} mb. On quenching the vacuum deteriorated momentarily to roughly 10^{-1}mb but recovered quickly.

Specimens were of full diameter bar stock, roughly 6" in length. Adsorbed surface layers were removed electrochemically to reduce contamination of the vacuum during heating to temperature and to permit more efficient hydrogen outgassing. Holes were drilled radially in the specimens at 30, 50 and 70mm from the bottom end to accommodate thermocouples. The specimen was secured in a zircaloy-2 collar at one end by means of a ¼" diameter zircaloy-2 pin passing through the specimen and collar. The purpose of the collar was to maintain the specimen centrally in the furnace tube and to ensure that the specimen was positioned correctly for quenching. The vertical position of the specimen in the furnace tube was monitored by means of a 'dummy' specimen outside the furnace.

Ageing of quenched bars was performed in a horizontal ageing furnace at a vacuum of better than 5×10^{-5}mb. The temperature of the specimen was monitored by a Pt/Pt-13Rh thermocouple in contact with the specimen. The temperature of the furnace was controllable to ± 4°C at 500°C.

4. RESULTS AND COMMENTS

4.1 The As-received Structure

The as-received material was relatively free of inclusions. A full chemical analysis is shown in Table 1. The principal impurity is silicon which is most probably concentrated in the glassy silicate inclusions which are occasionally observed. The only other impurities present at significant levels are Mg and Fe. As reported previously, the structure under polarised light consisted of an irregular α grain structure (Figure 3a). This bore little resemblance to the etched structure which consisted of eutectoid $\alpha + U_2Ti$ and residual areas between the eutectoid regions which had decomposed by nucleation and growth to a more equiaxed structure. (Figure 3b). The euctectoidal nature of the microstructure and the titanium distribution are clearly defined in the scanning electron micrograph and titanium linescan in Figures 4a and b. The as-received structure was consistent with that produced by slow cooling from γ. The lack of correspondence between polarised and etched structures resulted from the fact that while polarised light revealed the equilibrium room temperature α structure, the etched structure represented the titanium distribution established at higher temperatures.

The hardness of the as-received material varied from 336 Hv_{30} (± 10 Hv_{30}) at the front end of the extrusion to 314 Hv_{30} at the trailing end.

4.2 The Effect of Cooling Rate on Microstructure

After cooling from 780°C at between 2 and 10Ks^{-1}, the structure, viewed under polarised light, consisted of a mixture of equiaxed and lath-type α (Figure 5a). The orientation of the Widmanstätten-type α laths changed from one prior γ grain to another and was thus a function of prior γ orientation. A single phase delineation of the prior γ boundaries was often observed. After etching (Figure 5b) the structure consisted of laths of lamellar $\alpha + U_2Ti$

surrounding residual areas which had decomposed to a fine granular morphology. Very similar structures were observed after cooling from 880°C indicating that the microstructures were not significantly affected by holding temperature in the γ phase. The increase in cooling rate from 2 to 10 Ks^{-1} resulted in a slight increase in hardness from 311 Hv_{30} to 330 Hv_{30}. This change may not be significant since it is within the spread of values obtained from the as-received material.

Increasing the cooling rate to 30 Ks^{-1} produced a structure which, under polarised light, was comprised of fine, martensitic α' needles in a very fine granular α matrix (Figure 6). Etching revealed colonies of α' within the prior γ grain structure. A differential etching effect was apparent at prior γ grain boundaries. There was no evidence of a change of titanium content at the boundaries observed by titanium linescans in the scanning electron microscope. Under polarised light these regions were comprised of a fine granual α structure. A significant increase in hardness to approximately 394 Hv_{30} was obtained.

Further increases in cooling rate to 45, 98 and 170 Ks^{-1} resulted in progressive increases in the proportion of α' in the structures and a general coarsening of the martensitic plates until at a cooling rate of approximately 320 Ks^{-1} (Figure 7) the structure was almost entirely martensitic. However, the fine granular α persisted at prior γ boundaries. Similar structures were observed at 480 Ks^{-1} which was the highest cooling rate achieved in the present work.

The specimens quenched at 98, 320 and 480 Ks^{-1} were too thin to yield meaningful hardenss measurements. The hardness after quenching at 170 Ks^{-1} was approximately 414 Hv_{30} ($\pm$10 Hv_{30}) which is similar to that obtained after cooling at 45 Ks^{-1}.

In summary, very slow cooling rates (i.e. 2 Ks^{-1} or less) produced an equiaxed α structure under polarised light and a lamellar $\alpha + U_2Ti$ structure after etching. Slightly faster cooling induced a directionality in the granular α matrix which with further increase

TABLE 1. ANALYSIS OF AS-RECEIVED U-0.75 wt % Ti ALLOY

Element	Concentration (p.p.m. by atoms)
Ti	6,000*
Si	1,000
Mg	100
Fe	30
Ca	10
Al	10
Co	<1
Mn	3
S	10
P	<1
Zn	6
Cu	5
Cr	3
Ni	<3
K	3
U	Base

* This figure is unreliable since mass spectrometry is not accurate at these levels of Ti.

in cooling rate gave way to a martensitic α' structure with fine, granular α at prior γ boundaries.

4.3 Quenching of Full Size Bars

In order to characterise the microstructures obtained by cooling full size bars, and to relate these to the gas quenched structures, full size bars (35mm diameter) were quenched by various modes into oil.

i) Plunge Quenching

The microstructural regions resulting from plunge quenching a full size bar are shown in Figure 8a. The cooling rate was greatest at the end of the bar where initial contact was made with the quenchant. The microstructure in this region (Figure 9a and b), consisted almost entirely of coarse, martensitic α' with only occasional non-martensitic regions observed usually at prior γ grain boundaries. At a distance of approximately 8mm from the end of the bar the martensitic α' structure persisted. However, a refinement of the α' lath size and an increase in the amount of fine granular α at prior γ grain boundaries was observed (Figure 10a). Furthermore, towards the centre of this region, colonies of fine equiaxed α were observed which had initiated at prior γ grain boundaries (Figure 10b). This type of microstructure became more prominent with increase in distance from the end of the bar. Figures 11a and b show the structure close to the centre of the bar at 60mm from the bottom end. The measured cooling rate was approximately 70 Ks^{-1}. The microstructure consisted of α at prior γ boundaries with martensitic α' regions within the prior γ grains. Under polarised light the non-martensitic regions were of two forms; fine equiaxed granular regions and larger single phase regions such as that marked 'A' in Figure 11a. These two α morphologies may reflect different modes of transformation from γ. This point will be discussed in detail later.

Figure 12 shows evidence of star-shaped pores observed at a single localised region at the centre of the plunge quenched bar , 60mm

from the bottom end. Slight microstructural changes were evident in the vicinity of the defects. It is possible that these defects are a type of centreline void formed by quenching. It is also possible that they were caused by shrinkage porosity not healed by extrusion of the bar. This was the only observation of such defects during the present work.

The proportion of non-martensitic α decreased with increased distance from the centre of the bar. Figure 13 shows the structure close to the edge of the bar, 60mm from the bottom end. Although the structure was predominantly martensitic, a fine granular α delineation of prior γ grain boundaries was evident. With reference to the gas quenched microstructures, the structure shown in Figure 13 is consistent with a cooling rate of roughly 90 - 100 Ks^{-1}.

With the exception of the porosity defects, the structures observed at 60mm from the end of the bar were typical of those in the remainder of the bar.

In general, little variation in hardness of the plunge quenched bar was observed. The average hardness was 368 Hv_{30} (± 10 Hv_{30}) although a trend towards higher hardnesses e.g. 385 Hv_{30} towards the centre of the bar was noted. These higher hardnesses at the centre can be attributed to increased precipitation of U_2Ti during cooling.

ii) End Quenching

A full diameter bar 6" in length, was heated to 780°C and then cooled by immersion of one end in oil to a depth of 25mm. The rates of cooling at 700°C at the centreline of the bar, measured at distances of 30, 50 and 70 mm from the quenched end were 11 Ks^{-1}, 8 Ks^{-1} and 3 Ks^{-1} respectively. The bar could be divided into five micro-structural regions (Figure 8b). These were:-

1) The high cooling rate at the end of the bar which made initial contact with the quenchant was reflected in a coarse, almost fully martensitic α' structure with fine granular α occasionally observed at prior γ grain boundaries.

2) Between approximately 2 - 20mm from the quenched end the martensitic α' structure persisted but the granular α phase became more predominant at the prior γ boundaries, (see Figure 14), particularly near the centre of the bar. At 10mm from the quenched end very fine granular α was also observed between the α' laths within the prior γ grains, as in Figure 15.

3) The amount of non-martensitic α increased with distance from the quenched end of the bar until at 50mm from the quenched end the structure under polarised light consisted of a low volume fraction of fine α' laths within a granular α matrix (Figure 16a). Etching did not highlight the martensitic laths as in previous α' structures but instead the etched structure adopted a feathery appearance (Figure 16b and c) more reminiscent of the lamellar structures produced by slow cooling.

4) At greater distances from the quenched end of the bar the martensitic structure was replaced by a directional lath or Widmanstätten-type morphology, which existed within the coarsened granular α matrix, as shown in Figure 17a. On etching this structure adopted a feathery appearance together with regions which were more obviously eutectoidal, (Figure 17b).

5) Finally, at distances of 75mm and more from the quenched end the Widmanstätten-type structure gave way to a fully equiaxed α structure typical of that after very slow cooling rates in the as-received material.

The variation of hardness with distance in the end quenched bar is shown graphically in Figure 18. Up to a distance of 20 - 25mm from the quenched end the hardness was approximately 370 Hv_{30} (± 10 Hv_{30}). Between 25 and 40mm the hardness increased to approximately 395 Hv_{30} (± 10 Hv_{30}) after which it remained almost constant. The drop in hardness at higher cooling rates is most likely to be due to the retention of Ti in solution and suppresion of U_2Ti precipitation.

iii) Controlled Quenching at 100 mm/s.

A full diameter bar, 6" in length was heated to 780°C and immersed in oil at a rate of 100 mm/s. The resulting microstructural regions are shown diagrammatically in Figure 8c.

The region immediately adjacent to the end of the bar which made initial contact with the quenchant exhibited an almost fully martensitic α' structure. Prior γ grain boundaries were occasionally delineated by a fine granular α phase. This delineation became more prominent with increased distance from the end of the bar (Figure 19a) although most of the structure remained martensitic (Figure 19b). Finer laths within the coarse martensitic α' laths could be resolved at higher magnifications after etching, as in Figure 20. At a distance of roughly 30 - 35mm from the bottom end the α' lath size became more refined and more extensive regions of granular α were observed at prior γ grain boundaries. A typical structure is shown in Figure 21. At 50mm from the bottom end extensive colonies of granular α were observed (Figure 22). Martensitic areas persisted between the α colonies. This microstructure was typical of that in the remainder of the bar where the measured cooling rate was approximately 65 Ks^{-1}.

The variation in hardness with distance from the bottom of the bar is shown graphically in Figure 23. The hardness increased slightly from 340 to 370 Hv_{30} (±10 Hv_{30}) over the first 40mm from the end of the bar. Thereafter it remained almost constant at 370 - 380 Hv_{30} with increased distance from the end of the bar. This trend is similar to but less pronounced than that in the end quenched bar where the hardnesses were generally 20 - 30 Hv_{30} higher. This difference can be ascribed to the higher cooling rate in the controlled quenched bar and hence less precipitation of U_2Ti during the quench.

iv) Controlled Quenching at 10 mm/s.

The microstructural regions resulting from controlled quenching at an immersion rate of 10 mm/s are shown in Figure 8d. Microstructurally,

the bar was very similar to that quenched by immersion at 100mm/s except that the slower immersion rate (and hence slower cooling rate) promoted the formation of non-martensitic α. This manifested itself in a shift of all the microstructural zones towards the bottom end of the bar. Figures 24a and b are typical of the structure observed in the greater portion of the bar which was comprised of martensitic α' within prior γ grains and fine granular α in colonies and delineating prior γ grain boundaries. It is interesting to note that compared with the bar immersed at 100 mm/s, the rate of immersion of the present specimen was reduced by an order of magnitude but the cooling rate measured at similar points in the bars fell from approximately 65 Ks^{-1} to 50 Ks^{-1}.

The hardness variation in the bar immersed at 10 mm/s showed a similar trend to that in the bar immersed at the faster rate. The hardness rose from a value of approximately 350 Hv_{30} to the end of the bar and remained almost constant at 370 Hv_{30} at distances greater than 25mm from the end.

4.4 The Effect of Ageing

Previous work[11,12] has indicated that peak hardness in the present alloy can be achieved by ageing for approximately 3 hours at 450°C. The end quenched bar specimen was therefore given this ageing treatment in order to determine the effect of ageing on the full range of microstructures. A second bar, controlled quenched at 100mm/s, was also aged with a view to determining the hardening response obtainable in bars oil quenched after γ extrusion.

i) Ageing of End Quenched Bars

Ageing of the end quenched bar for 3 hours at 450°C had little discernible effect upon the optical microstructure. As in the unaged bar, the structure, up to approximately 50mm from the quenched end, consisted of a mixture of martensitic α' and fine granular α ; the latter being usually associated with prior γ grain boundaries. Figure 25 shows a typical microstructure. At greater distances from the end of the bar the microstructure adopted a Widmanstätten

appearance (Figure 26) which, with increased distance, gave way to an equiaxed granular α structure.

The variation in hardness with distance in the bar after ageing is shown in Figure 18 where it is compared with the unaged hardness. Hardnesses in the region of 460 - 490 Hv_{30} were achieved in the first 20 - 30mm of the specimen. At greater distances from the quenched end the hardness dropped to approximately 390 - 400 Hv_{30}. By comparison with the unaged hardness it is seen that at a distance of 30mm and over, little or no hardening was achieved by ageing at 450°C. However, in regions of the specimen where the quench rate was sufficiently high to retain appreciable amounts of titanium in solution (i.e. at less than 30mm from the quenched end), an increase in hardness of approximately 100 Hv_{30} was achieved. It is concluded that while only comparatively low hardnesses can be achieved by the retention of titanium in solution, the hardness can be considerably increased by the precipitation of titanium in the form of U_2Ti.

ii) Ageing of Bar Controlled Quenched at 100 mm/s.

Ageing of the end quenched bar indicated that a sufficiently high cooling rate achieved thoughout a bar would result in a good hardening response on subsequent ageing. The bar quenched by immersion in oil at 100 mm/s was therefore aged for 3 hours at 450°C. By comparison with the unaged bar, little change in microstructure resulted from ageing although some evidence suggested that the granular α regions at prior γ grain boundaries were slightly more extensive after ageing. This was difficult to quantify.

The variation of hardness with distance in the bar after ageing is shown in Figure 23. Close to the end of the bar where the initial quench rate was highest ageing resulted in an increase in hardness from 340 to 520 Hv_{30}. In most of the bar, where the cooling rate had stabilised at approximately 65 Ks^{-1}, (measured on the centreline of the bar) ageing produced a hardness of between 470 and 480 Hv_{30} which represented an increase of approximately 100 Hv_{30} over the as-quenched material.

TABLE 2 : RESULTS OF X-RAY EXAMINATION

HEAT TREATMENT	b (Å)	COMPOSITION (At.% Ti)	TEXTURE COEFFICIENTS OF FIVE MOST PROMINENT PLANES					COMMENT
As received	5.858	1.8** 0.6+	(002) 3.2	(021) 2.8	(111) 2.4	(110) 0.6	(040) 0.2	Sharp U_2Ti peaks. No α_1/α_2 resolution.
Radiation cooled from 780°C @ 2 Ks^{-1}	5.857	1.9 0.7	(002) 0.8	(021) 1.3	(111) 0.7	(200) 0.9	(040) 0.9	Sharp U_2Ti peaks. Partial α_1/α_2 resolution.
Radiation cooled from 880°C @ 2 Ks^{-1}	5.857	1.9 0.7	(002) 1.5	(021) 1.4	(111) 1.3	(200) 0.9	(110) 0.9	As above
Gas quenched from 780°C @ 100-300 Ks^{-1}	5.846	2.8 1.8	(002) 0.7	(021) 0.6	(111) 0.7	(130) 2.1	(113) 2.4	Very weak U_2Ti peaks. No α_1/α_2 resolution.
Bar, plunge quenched from 780°C	5.850	2.4 1.3	(002) 2.0	(021) 1.9	(111) 1.2	(130 0.9	(042) 2.2	Very weak U_2Ti peaks. No α_1/α_2 resolution. Examined 60mm from bottom end. ($\sim$70 Ks^{-1})
Bar, end quenched from 780°C	5.854	2.1 1.0	(002) 2.1	(021) 1.5	(111) 1.3	(130) 0.9	(042) 1.7	Weak U_2Ti peaks. No α_1/α_2 resolution. Examined 60mm from end. ($\sim$6 Ks^{-1})
Bar, control quenched from 780°C Immersion rate 100 mm/s	5.846	2.8 1.8	(002) 1.3	(021) 2.0	(111) 1.5	(130) 1.6	(042) 1.5	Very weak U_2Ti peaks. No α_1/α_2 resolution. Examined 15mm from bottom end. ($\sim$80 Ks^{-1})
Bar, control quenched from 780°C Immersion rate 10 mm/s	5.851	2.3 1.2	(002) 0.9	(021) 1.1	(111) 1.5	(130) 1.3	(042) 0.9	As above

+ Compositions obtained using lattice parameter/composition curves due to Anagnostidis et al (13)
** " " " " " " " " Douglass (14)

NOTE : All specimens were examined with surfaces perpendicular to extrusion direction.

4.5 X-Ray Diffraction Studies

Selected specimens were examined by X-ray diffraction in order to determine:-

a) preferred orientation

and b) amount of titanium in solid solution by 'b' lattice parameter determination.

The preferred orientation of samples was investigated by determining texture coefficients (TC) for diffraction peaks using the expression:

$$TC = \left(I/I_o\right)_{hk\ell} \Big/ \frac{1}{n}\sum\left(I/I_o\right)_{hk\ell}$$

in which I is the observed height of the hkℓ peak

I_o is the corresponding intensity for a random sample

and n is the number of diffraction peaks employed in the analysis.

A texture coefficient is proportional to the volume amount of material which is oriented with an {hkℓ} plane parallel to the surface of the sample. The sample surfaces examined were perpendicular to the long direction of the bar. Hence the texture coefficient so obtained revealed the way in which the α was orientated relative to a plane perpendicular to the extrusion direction, i.e. the orientation of α along the extrusion direction.

The results of the X-ray examinations are shown in Table 2. A pronounced (002) texture was observed in the as-received material which had been γ extruded. Subsequent reheating into γ and cooling at various rates between 2 Ks^{-1} and 300 Ks^{-1}, destroyed or reduced this (002) texture. No strongly preferred orientation was observed in any of the specimens examined. Slow cooling from 780°C at 2 Ks^{-1} produced an almost random structure while cooling at the same rate from 880°C produced a slightly more prominent (002) texture

although this was still relatively weak. Increased cooling rate to between 100 and 300 Ks^{-1} produced prominent (130) and (113) textures. Quenching of bar specimens did not produce strongly pronounced textures although (021) and/or (002) were prominent in these specimens.

The 'b' lattice parameter of uranium is the most sensitive to solute content and decreases with increased titanium in solution. The accepted 'b' lattice parameter for pure uranium is 5.868Å while that of U-¾ wt % Ti, with all the titanium in solution, is either 5.820Å or 5.828Å, depending upon whether the data of Anagnostidis et al[13] or Douglass[14] respectively is used. The data from these two sources are plotted for comparison in Figure 27. The reason for the discrepancy in the curves is not obvious. Anagnostidis et al heat treated <2mm thick slices in vacuum followed by water quenching after back-filling the system with argon. Douglass used encapsulated wafers which were quenched into water. Neither quench rate nor specimen thickness is known but no evidence of U_2Ti formation was detected. It is known that at high quench rates and a given solute content the 'b' lattice parameter can increase with increasing quench rate. Hence the discrepancy may be due to a difference in quench rates.

The discrepancy could also be due to differing effective solute contents e.g. some titanium could have been removed from solution as insoluble TiC by reaction with carbon impurities. Unfortunately, accurate chemical analyses are not available and in the absence of more detail of experimental methods is is impossible to resolve the discrepancies between the two sets of data.

In the present work the level of titanium retained in solution was lowest in the as-received and slow cooled materials. The presence of sharp U_2Ti diffractions from these specimens confirmed that titanium had precipitated from solution during the slow cool from γ. At faster cooling rates only very weak U_2Ti diffractions were observed and the level of titanium retained in solution was generally higher. The general absence of α_1/α_2 peak resolution can be ascribed to lattice strains resulting from precipitation of U_2Ti, quenching strains (i.e. transformation strains), or possibly titanium retained in solution.

5. GENERAL DISCUSSION

It has been shown that the room temperature microstructure of U-¼% Ti is a sensitive function of cooling rate from the γ phase. From the gas quenching experiments it has been determined that the significant quench rates are:-

a) <2 Ks^{-1}. At the slowest rate of cooling from γ the structure consists crystallographically of equiaxed granular α, as revealed by polarised light. Etching, which reveals the 'chemical structure', produces a eutectoidal microstructure reflecting the titanium distribution established at higher temperatures.

b) 2 - 30 Ks^{-1}. Cooling rates between 2 and 10 Ks^{-1} result in structures comprised of oriented laths of Widmanstätten-like α in an equiaxed granular α matrix. The directionality of the Widmanstätten-type structure becomes increasingly pronounced as the cooling rate is increased to approximately 30 Ks^{-1}.

c) 30 Ks^{-1} upwards. At cooling rates in the region of 30 Ks^{-1} martensitic α' needles are observed within a granular α matrix. As the cooling rate is increased the martensitic structure becomes increasingly predominant until at quench rates in excess of ~100 Ks^{-1} the structure is almost fully martensitic. However, a fine granular α delineation of the prior γ grain boundaries persists even at cooling rates in the region of 480 Ks^{-1}. This fine granular α phase is assumed to have been formed by nucleation and growth during the quench.

Neither metallography or X-ray examination revealed any evidence of β phase retention at room temperature, regardless of cooling rate. The rôle of β phase in the $\gamma \rightarrow \alpha$ decomposition must therefore be deduced by reference to room temperature microstructures. At very slow cooling rates β formed initially from γ by nucleation and growth.

Depression of the $\gamma \rightarrow \beta + U_2Ti$ eutectoid temperature resulted in a higher proportion of β in the structure than would be expected under equilibrium cooling conditions. The structure thus consisted of areas of β surrounding residual γ regions which subsequently transformed to $\beta + U_2Ti$. On further cooling α nucleated from β and grew to form the roughly equiaxed structure observed under polarised light.

A similar sequence of precipitation occurred at slightly faster cooling rates except that a Widmanstätten-type lath precipitation of β from γ was induced. Furthermore, the residual γ regions may have transformed directly from γ to $\alpha + U_2Ti$ producing a granular or fine lamellar structure.

At higher cooling rates (i.e. in excess of 30 Ks^{-1}) martensitic α' needles were observed. This indicated that transformation from α to β was suppressed to below the M_s temperature of 615°C, determined by Eckelmeyer and Zanner[15], and the fine granular α matrix was formed directly from γ. On etching this matrix appeared featureless, in contrast to the eutectoidal appearance associated with slower cooled microstructures. This was indicative of the fact that at higher quench rates a higher proportion of titanium was retained in solution where its distribution was approximately uniform. This argument is supported by the results of the X-ray examination which confirmed that a large proportion of titanium remained in solution after the faster quenches. For instance, after quenching at approximately 100 Ks^{-1} or more, approximately ½ - ¾ of the available titanium was retained in solution. (Note: 0.75 wt % Ti $\simeq$ 4 at % Ti).

The above levels of titanium retention would result in a considerable increase in mechanical properties if the titanium were precipitated as U_2Ti by low temperature ageing. In Appendix A it has been assumed that 2 at % titanium is precipitated as U_2Ti. It is shown that this would result in a precipitate volume fraction of roughly 0.05. Assuming that this precipitate is uniformly distributed throughout the matrix in the form of 100Å diameter spheres, it is shown that the average distance of closest approach of the particles is

approximately 20Å. If the particles were coarsened to 500Å the average distance between particles would be approximately 80Å. This would be expected to result in significant levels of strengthening.

The above predictions are borne out by the results of ageing treatments on end quenched and controlled quenched bars. With reference to the end quenched bar, hardness measurements indicated that only a comparatively low level of strengthening could be achieved by retaining titanium in solution. However, in regions of the bar where a lower quench rate had resulted in precipitation of U_2Ti during the quench, a slightly higher hardness was achieved. After ageing this situation was reversed. The highest hardness was obtained in regions of the bar which had retained most titanium in solution during quenching, (see Figure 18). Very little age hardening occurred in regions where U_2Ti had precipitated during the quench. However, X-ray examination of the slower cooled regions of the end quenched bar indicated that between 1 - 2 at % titanium remained in solution after quenching, (see Table 2). This level of titanium should produce significant levels of precipitation hardening. The fact that no precipitation hardening was obtained in the slower cooled regions of the bar (Figure 18) suggests that exsolution of the titanium during ageing promoted growth or overageing of the existing precipitates rather than the nucleation of a fine distribution of U_2Ti.

The X-ray results indicated that between 2 and 3 at % titanium was retained in solution in the bar quenched at an immersion rate of 100 mm/s. Ageing resulted in a general increase in hardness of typically 120 - 130 Vickers hardness points to approximately 475 Hv_{30}, although larger increases were observed near the end of the bar where the initial cooling rate was greatest. The significance of these results is two-fold. Firstly, they confirm that hardnesses in excess of 480 Hv_{30} are obtainable in these bars. A series of isothermal and isochronal experiments should now be carried out on similarly quenched bars in order to determine the optimum ageing treatment. Secondly, they show that full diameter bars can be quenched at a sufficiently high rate to give a good hardening response on

subsequent ageing, yet without inducing quench cracking or centreline void formation. The negative volume change associated with the $\gamma \rightarrow \alpha$ transformation in U-Ti can produce sufficiently high stresses in quenched rods to result in the above types of defects[12,16]. For example, after water quenching a bar 1⅜" diameter x 4" long from 800°C, Ammons[12] has measured residual tensile stresses of 110 and 85 ksi in the longitudinal and tangential directions respectively. Anderson[16] has also observed large centreline voids in 1½" diameter U-¾ Ti bar similarly quenched.

In the present work the only evidence of centreline defects observed were pores at a single position in the plunge quenched bar. These pores were not observed in a region of the bar which had undergone the highest rate of cooling and it is considered more likely that they resulted from shrinkage during or immediately after γ phase extrusion rather than from quenching effects. These defects apart, no evidence of quench-induced centreline defects was observed in any of the specimens. This can be ascribed to the moderate quench rates obtained by oil quenching rather than water quenching.

The γ extruded, as-recieved material exhibited a prominent texture with (002) perpendicular to the extrusion direction. (021) and (111) textures were also prominent. These textures could be partially destroyed by reheating into the γ field followed by quenching at up to approximately 300 Ks^{-1} which produced almost random orientation. Pronounced textures were not induced by controlled immersion at 100 mm/s or 10 mm/s. This is somewhat surprising since in other work an α-extruded U-¾ Ti[17] in the form of 30mm diameter bar the (002) extrusion texture was replaced by a prominent (200) transformation texture after controlled immersion. Further effort is required to produce more prominent transformation textures in the present bars. The desirability of inducing certain textures in uranium and its alloys arises from the fact that at room temperature there exists only one easy slip system[18] i.e. (010) [100], and it has been found possible to achieve significant levels of texture strengthening. For instance,

while the Young's modulus of nontextured, polycrystalline, pure α-uranium is 29 x 10^{-6} lbf.in^{-2} at room temperature it can be varied between 21 x 10^{-6} and 41 x 10^{-6} lbf.in^{-2} by suitable texturing[19,20].

6. CONCLUSIONS

The following conclusions are drawn from the present work:-

i) The as-received material has a roughly equiaxed, granular α structure with U_2Ti distributed as particles in one phase of a fine lamellar structure. The structure is consistent with that expected in a material slow cooled from the γ phase subsequent to final processing.

The material has a relatively low inclusion content, most of which were in the form of glassy silicates.

ii) Cooling rates from the γ phase have been varied between 2 and 480 Ks^{-1}. This resulted in microstructures ranging from granular α after slow cooling to almost fully martensitic α' at the higher cooling rates. The fine grained α produced by the slowest cooling rates bore little relationship to the eutectoid-like structure found on etching. At slightly increased rates of cooling oriented laths of α(probably derived from the β phase) existed within prior γ grains, the remainder of which had transformed to a roughly equiaxed α structure. At quenching rates in excess of approximately 30 Ks^{-1} increasingly greater proportions of martensitic α' were observed in a granular α matrix.

iii) The general absence of centreline cracking or void formation is attributed to the moderate quench rates which are, nevertheless, sufficiently high to retain approximately half of the available titanium in solution.

iv) Ageing resulted in marked increases in hardness to approximately 480 Hv_{30} generally, with higher values (up to 520 Hv_{30}) in regions where the initial quench rate was highest.

v) A pronounced (002) texture existed in the as-received material. This persisted, but was much less pronounced, after reheating into the γ phase field and cooling at any rate.

Strong transformation textures were not produced by controlled immersion quenching at rates of immersion of 10 or 100 mm/s. However, (002), (021) and (111) textures were generally prominent in these specimens. Furthermore, other work on a similar alloy extruded in the α phase has shown that more pronounced textures can be induced by controlled quenching at certain rates of immersion.

7. REFERENCES

1. Sandstrom, D.J. In "Proc of High Density Alloy Penetrator Materials Conf.", AMMRC., Watertown, USA, 1977, P 419.

2. Buzzard, R.W., Liss, R.B., Fickle, D.P.., J.Res.Nat.Bur.Stand., 50, (4), 209, 1953.

3. Udy, M.C., Boulger, F.W., Trans. A.I.M.E., 200, 207 & 1317, 1954.

4. Udy, M.C., Boulger, F.W., Report BMI 774, U.S. Atomic Energy Commission Publicn. 1952.

5. Knapton, A.G., J.I.M., 83, 497, 1954.

6. Adda, Y., Beyeler, M., Kirianendo, A., Maurice, R., Mem.Sci.Rev.Met. 58, 716, 1961.

7. Howlett, B.W., Knapton, A.G., In "Proc 2nd UN Int.Conf. on Peaceful Uses of Atomic Energy", 6, Geneva, 1958, p 104.

8. Linard, M., U.S. Atomic Energy Commission Report ORNO-tr-2579, July 1971.

9. Lehmann, Mme. J., Hills, R.F., J.Nuc.Mat., 2, (3), 261, 1960.

10. Saunderson, R.I., Brook, G.B., F.R.I. Report R812/3. This Contract, August 1980.

11. Eckelmeyer, K.H., "Ageing Phenomena in Dilute Uranium Alloys" in "Physical Metallurgy of Uranium Alloys", ed. Burke, J.J. et al., Brook Hill, 1976, P463.

12. Ammons, A.M., "Precipitation Hardening in Uranium Rich Uranium Alloys". IBID, P511.

13. Anagnostidis, M., Bauschwitz, R., Colombie, M., Mem.Sci. Rev.Met., 63, 163, 1966.

14. Douglass, D.L., Trans. A.S.M. 53, 307, 1961.

15. Eckelmeyer, K.H., Zanner, R.J., J. Nuc.Mat., 67. 33, 1977.

16. Anderson, R.C., Unpublished Work, Cited as Ref. 25 in Ref. 12.

17. Saunderson, R.I., Brook, G.B., Unpublished Work, Fulmer Research Institute, 1981.

18. Yoo, M.H., J. Nuc.Mat., 26, 307, 1968.

19. Armstrong, P.E., Eash, D.T., Hockett, J.E., J. Nuc.Mat., 45, 211, 1972.

20. Fisher, E.S., J. Nuc.Mat., 18, 39. 1966.

21. Pearson, W.B., "Handbook of Lattice Spacings and Structures of Metals", Vol. 1, p 874, Permagon Press, 1958.

22. Hertz, P., Math.Ann., 67, 387, 1909.

23. Chandrasekhar, S., Rev.Mod.Phys., 15, 1943.

APPENDIX A

CALCULATION OF NUMBER AND DISPERSION OF U_2Ti PARTICLES CORRESPONDING TO PRECIPITATION OF 2at%Ti FROM URANIUM

It is assumed that 2at%Ti is precipitated from solution in the form of stoichiometric U_2Ti.

Parameters of U_2Ti unit cell [21]

Hexagonal $a = 4.828\text{Å}$ $c = 2.847\text{Å}$

Volume of unit cell $= \sqrt{3}/2\ a^2c$

$= 0.866(4.828)^2 \times 2.847 \times 10^{-24}\ cm^3$

Number of U_2Ti unit cells

For 2at%Ti, number of unit cells =

$$\frac{2\rho N}{100 \times \text{AT. WT. U}} \quad \text{cells cm}^{-3}$$

where N = Avagadro's number

ρ = density of uranium = 19.05 gm cm^{-3}

Hence,

$$\text{number of cells} = \frac{2 \times 19.05 \times 6.0235 \times 10^{23}}{100 \times 238.03}$$

$$= \frac{3.81 \times 6.0235 \times 10^{24}}{2.3803 \times 10^4} \text{ cells cm}^{-3}$$

Total volume of U_2Ti precipitate corresponding to 2at%Ti

Total volume of cells = Volume/cell x Number of cells

$$= 0.866(4.828)^2 \times 2.847 \times 10^{-24} \times \frac{3.81 \times 6.0235 \times 10^{24}}{2.3803 \times 10^4}$$

$$= 5.541 \times 10^{-2}\ cm^3$$

Now assume that the above volume of U_2Ti precipitate is uniformly distributed in the form of spherical particles 100Å in diameter.

Volume of 100Å diameter sphere $= {}^4/_3\ \pi\ r^3$

$$= \pi/6 \times 10^{-18}\ cm^3$$

$$\text{Number of precipitates/cm}^3 = N_v = \frac{\text{Total volume to be precipitated}}{\text{Volume/particle}}$$

$$\approx 10.6 \times 10^{16} \approx 10^{17}\ cm^{-3}$$

Average distance between precipitate centres

Following Hertz [22] and Chandrasekhar [23], the average distance, $\bar{\lambda}$, between randomly distributed particle centres in a volume, V, is given by:

$$\bar{\lambda}_v = 0.554\ N_v^{-1/3}$$

$$= 0.177 \times 10^{-5}\ \text{cm}$$

$$\simeq 120\text{Å}$$

Hence for 100Å diameter speheres the average distance of closest approach is 20Å.

If the sphere diameter is increased to 500Å the above calculation can be repeated to predict an average distance of closest approach of approximately 80Å.

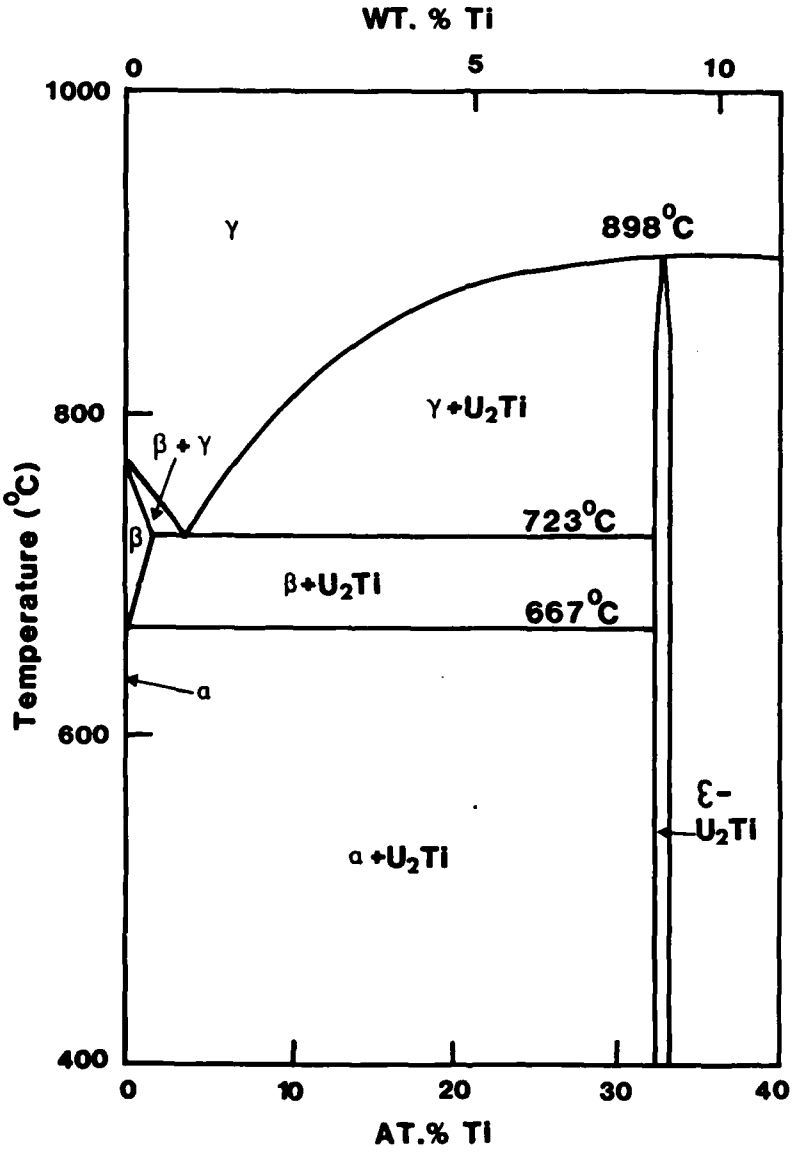

Figure 1 The uranium-rich portion of the uranium- titanium phase diagram, after Knapton(5)

Note: 3/4 WT. % Ti ≃ 4 AT. % Ti

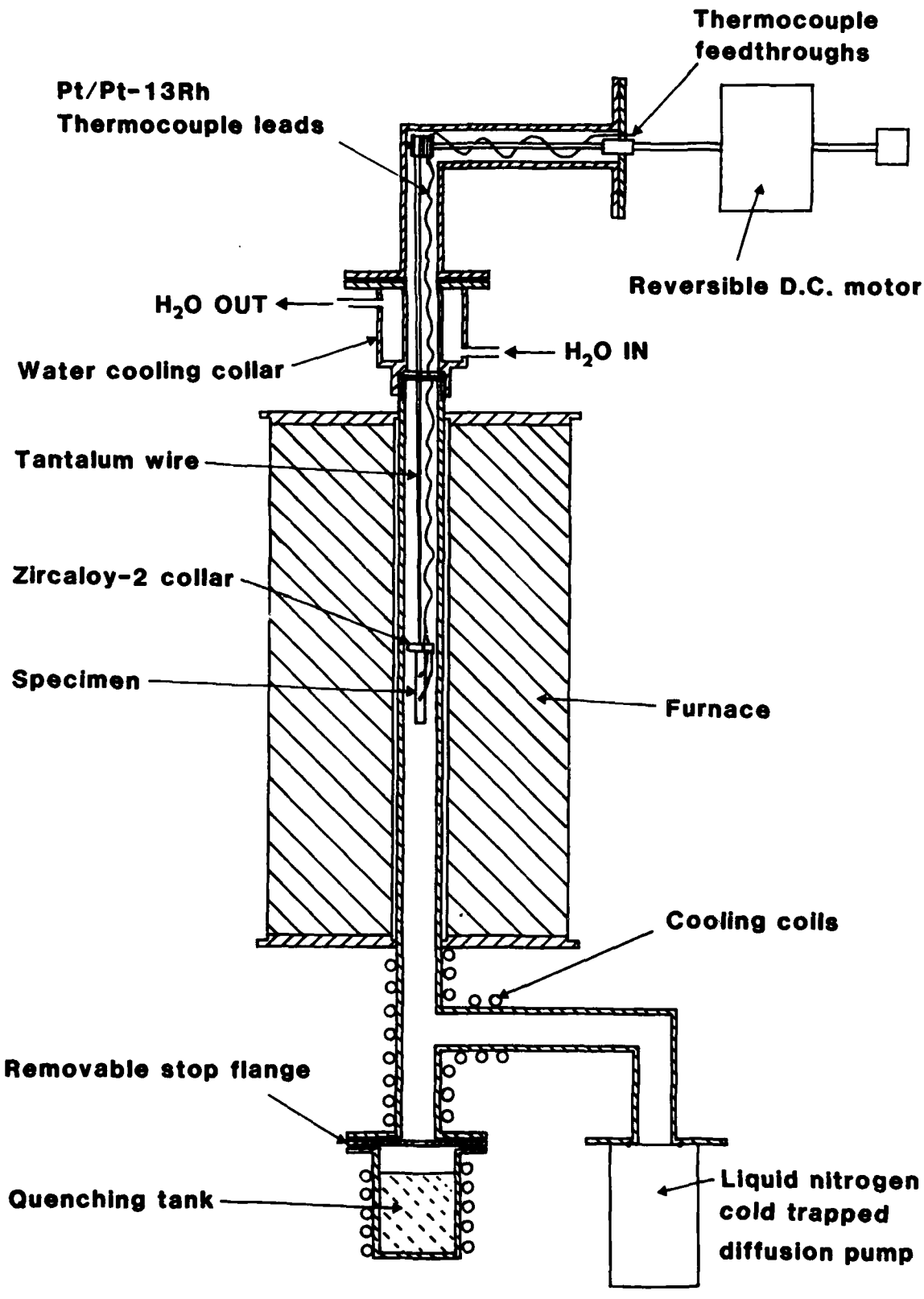

Figure 2 . Diagram of vertical quenching furnace

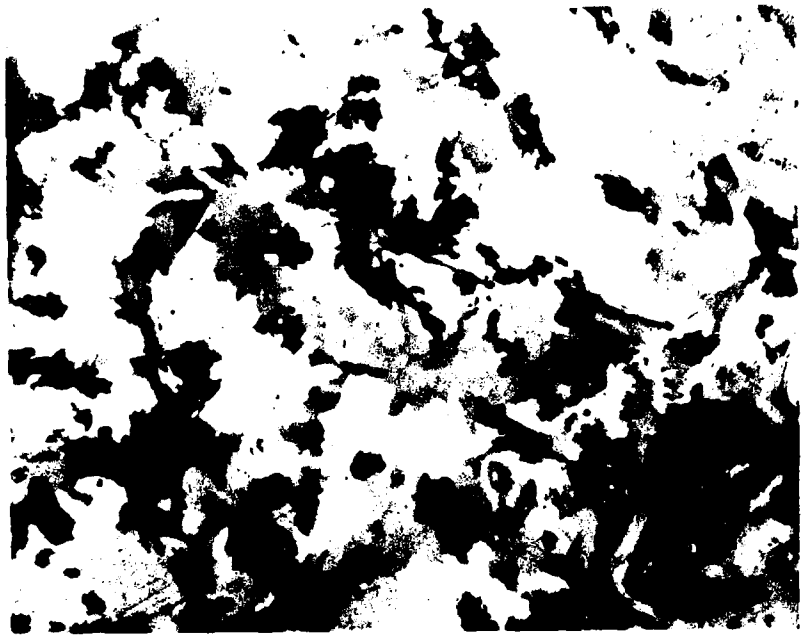

Figure 3a. CROSSED POLARS x 150
F4680

Figure 3b. ETCHED (BRIGHT FIELD) x 150
F4681

Figure 3. Microstructure of as-received material.

R812/4

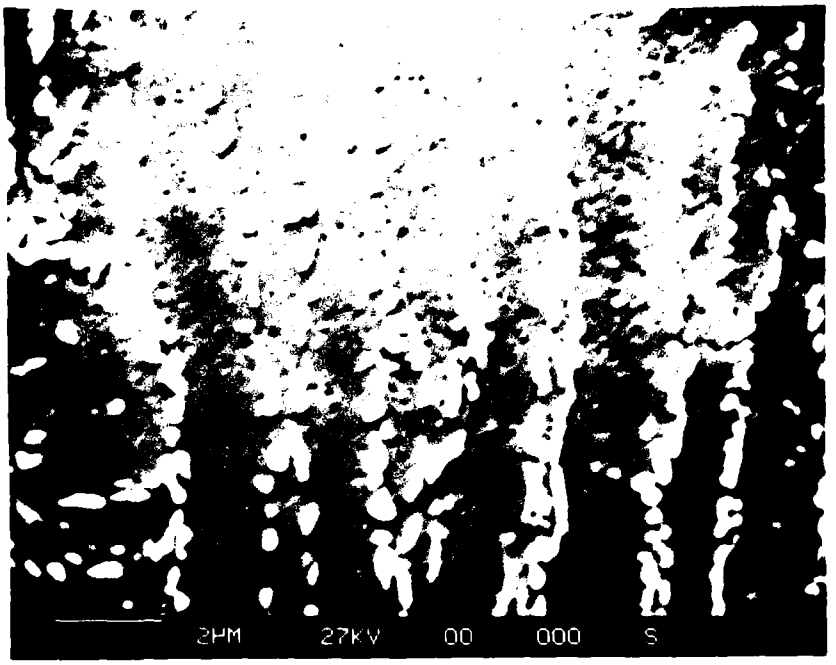

Figure 4a. PO304

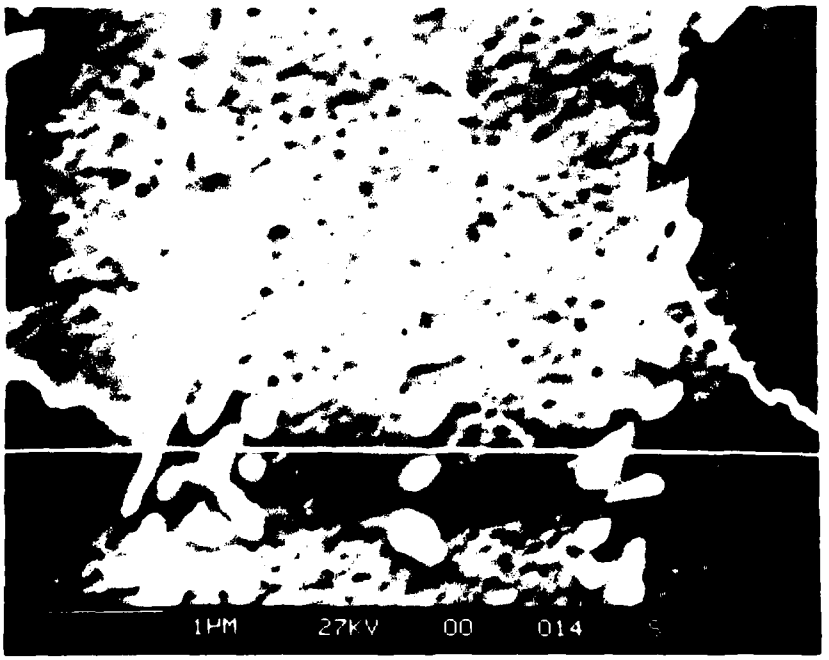

Figure 4b. PO305

Figure 4. Scanning electron micrograph (Figure 4a) and linescan for titanium (Figure 4b) from as-received material.

R812/4

Figure 5a. CROSSED POLARS x 150
F3797

Figure 5b. ETCHED (BRIGHT FIELD) x 150
F3798

Figure 5. Showing the microstructure after cooling at $10KS^{-1}$.

R812/4

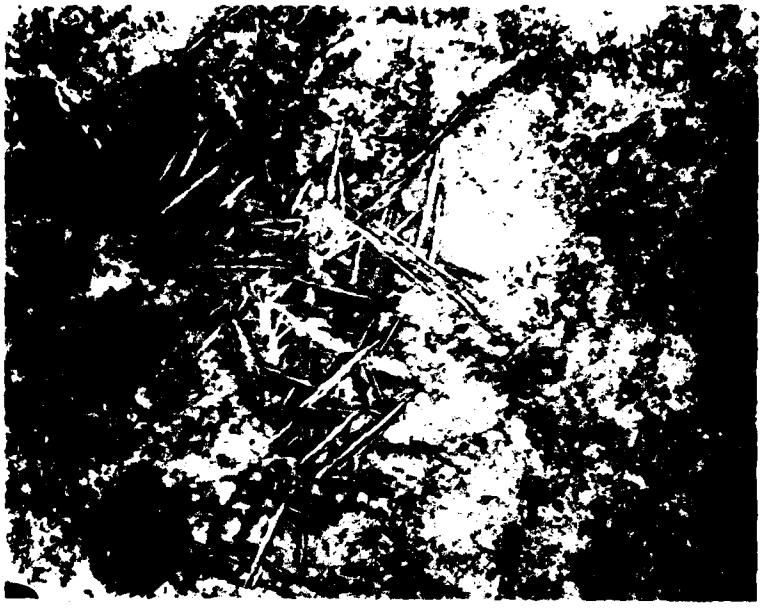

Figure 6. Showing microstructure after cooling at 30 Ks^{-1}. ETCHED AND CROSSED POLARS x 150 F3911

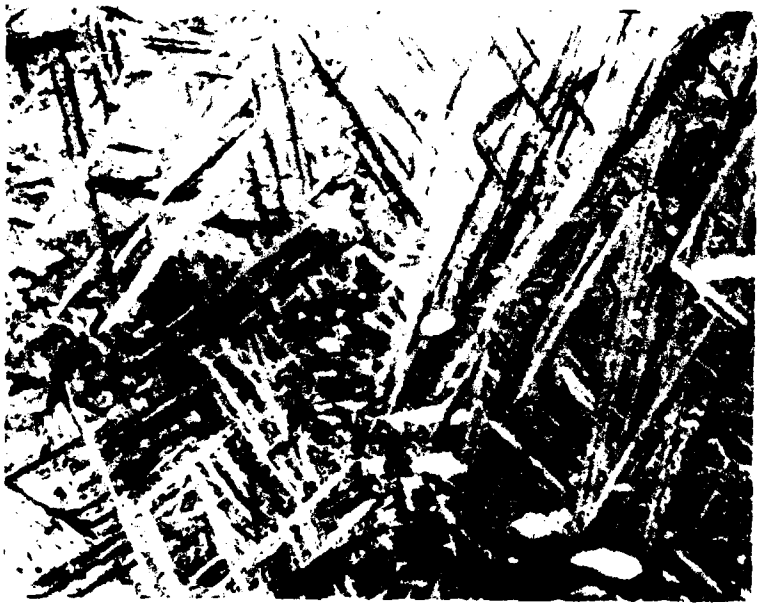

Figure 7. Showing microstructure after cooling at 320 Ks^{-1}. CROSSED POLARS x 150 R3761

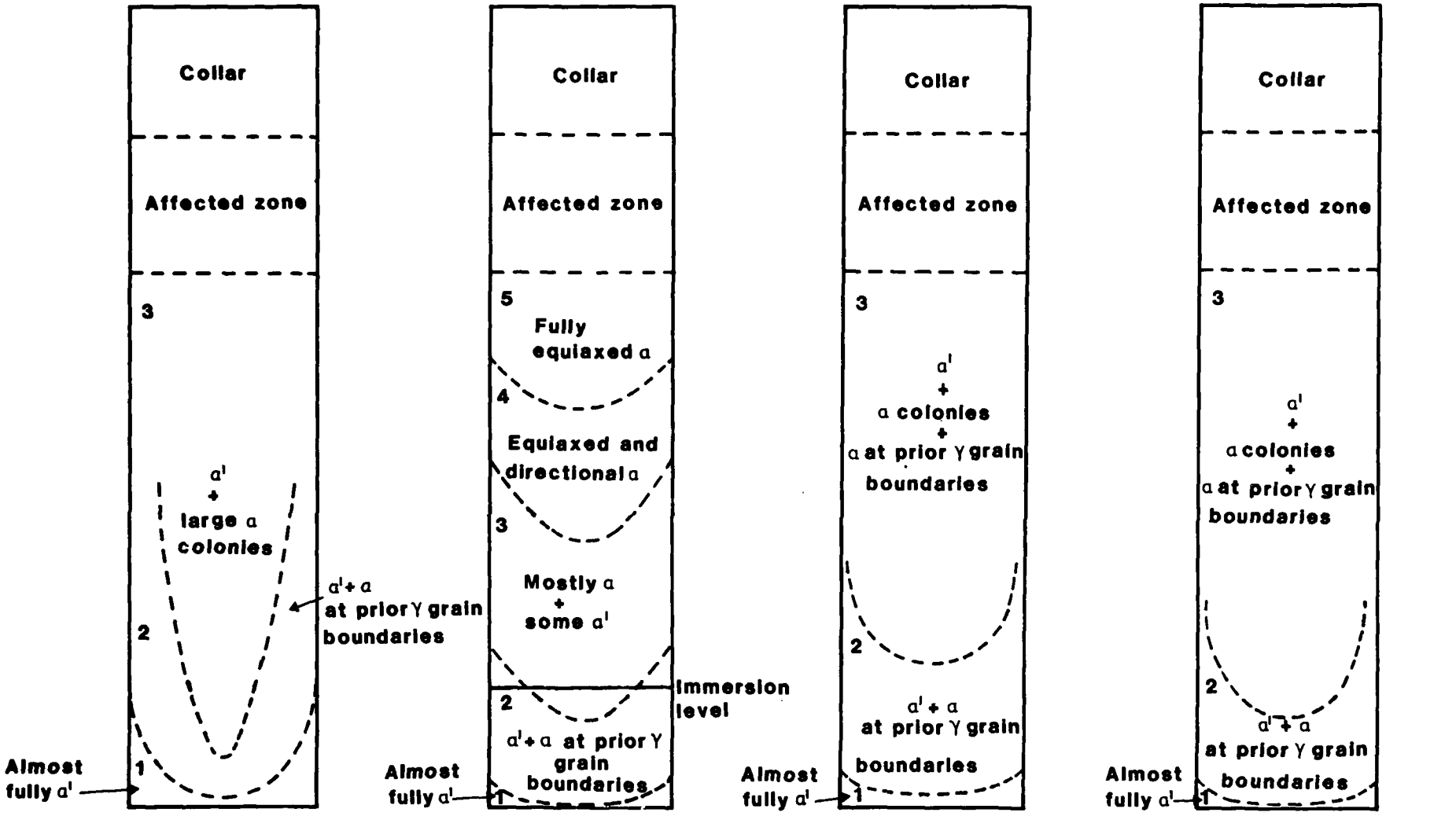

(a) Plunge quench

(b) End quench

(c) Controlled quench
(Immersed at 100mm/s)

(d) Controlled quench
(Immersed at 10mm/s)

Figure 8 Microstructual regions in quenched bars

Scale :full size

Figure 9a. CROSSED POLARS x 150
F4654

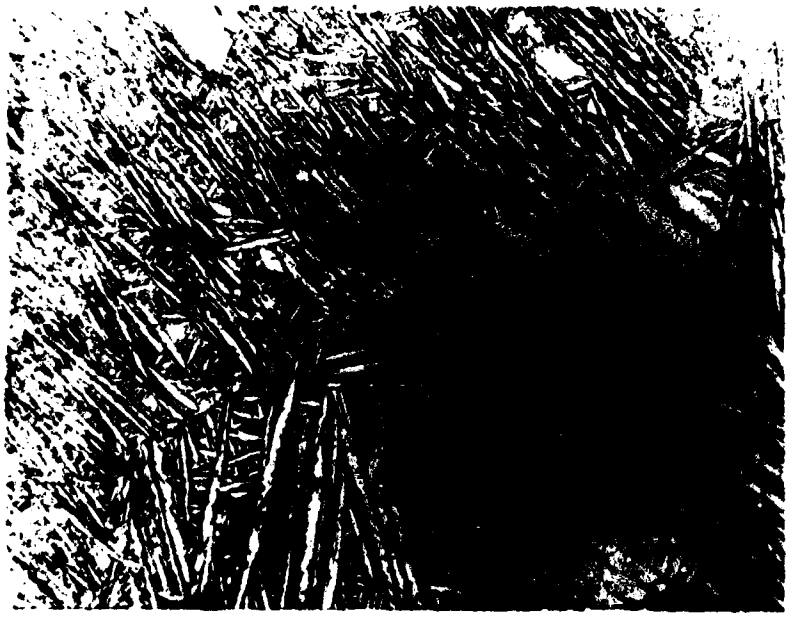

Figure 9b. ETCHED (BRIGHT FIELD) x 150
F4658

Figure 9. Showing general microstructure 2mm from end of of plunge quenched bar.

R812/4

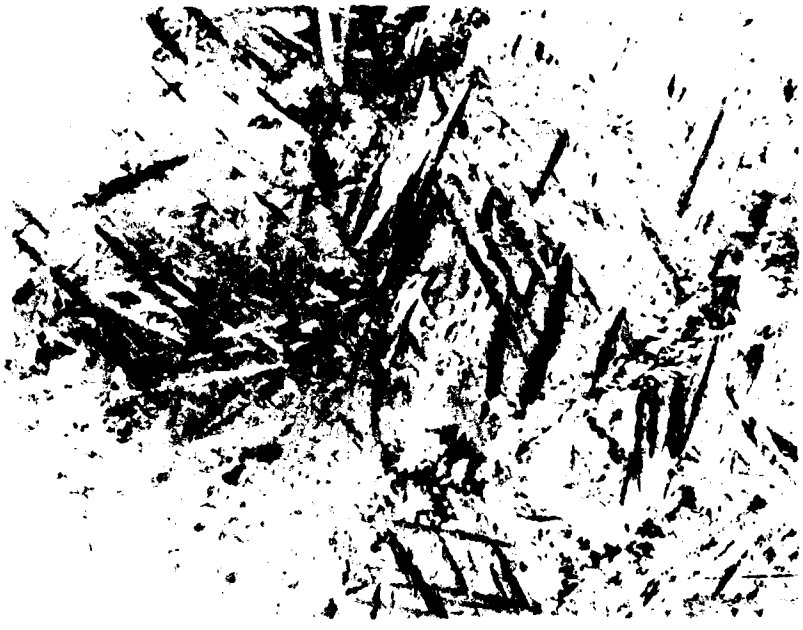

Figure 10a. CROSSED POLARS x 150
F4657

Figure 10b. ETCHED (BRIGHT FIELD) x 150
F4659

Figure 10. Showing microstructure 8mm from bottom end of plunge quenched bar. R812/4

Figure 11a. CROSSED POLARS x 150
F4650

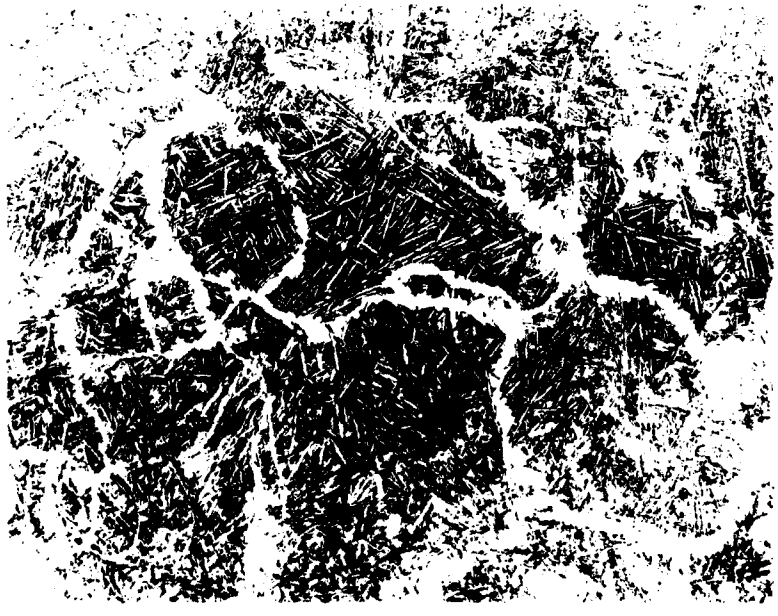

Figure 11b. ETCHED (BRIGHT FIELD) x 50
N9237

Figure 11. Showing general microstructure 60mm from bottom end of plunge quenched bar. Note the single phase delineation of prior γ grain boundary, marked 'A' in Figure 11a. R812/4

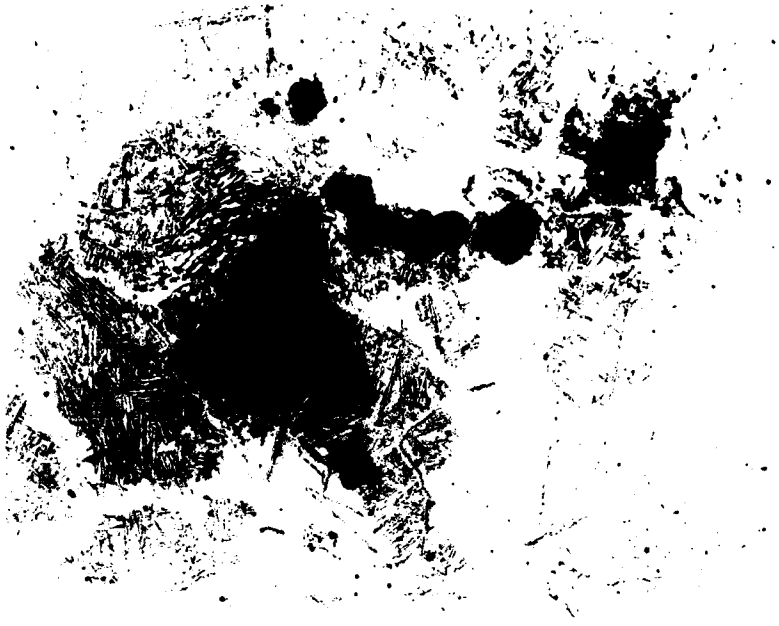

Figure 12. Showing pores near centreline of plunge quenched bar, 60mm from bottom end. x 150 N9056
ETCHED (BRIGHT FIELD)

Figure 13. Showing martensitic α' microstructure close to outer edge, 60mm from bottom end of plunge quenched bar. x 150 F4649
CROSSED POLARS R812/4

Figure 14. Showing microstructure 2 mm from end of end quenched bar. Note the granular nature of the regions adjacent to prior γ grain boundaries. x 150 F4253
ETCHED + CROSSED POLARS

Figure 15. Showing microstructures 10mm from end of end quenched bar. x 150 F4212
ETCHED + CROSSED POLARS

Figure 16a.

CROSSED POLARS

x 150

F4224

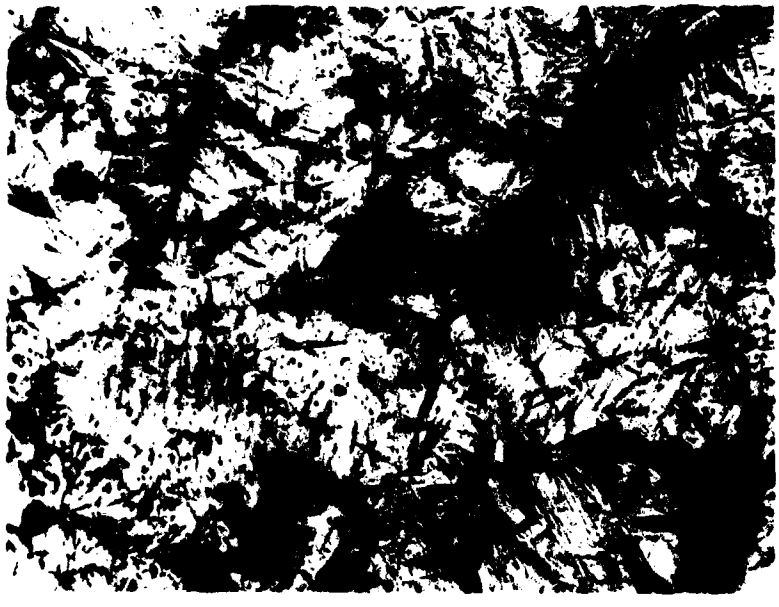

Figure 16b.

ETCHED

(BRIGHT FIELD)

x 150

F4257

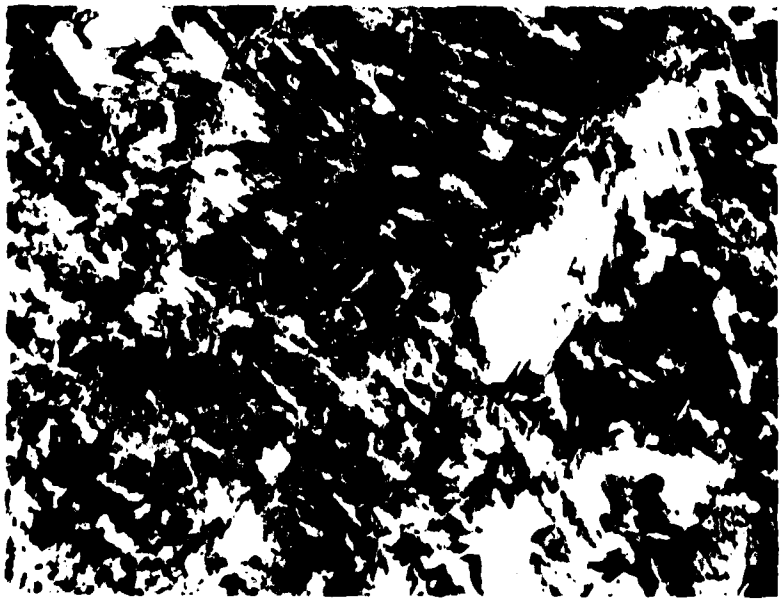

Figure 16c.

ETCHED +

CROSSED POLARS

x 150

F4258

Figure 16. Showing microstructure 50mm from end of end quenched bars.

R812/4

Figure 17a. CROSSED POLARS x 150
F4671

Figure 17b. ETCHED (BRIGHT FIELD) x 150
F4259

Figure 17. Showing microstructure 70mm from end of end quenched bar.

R812/4

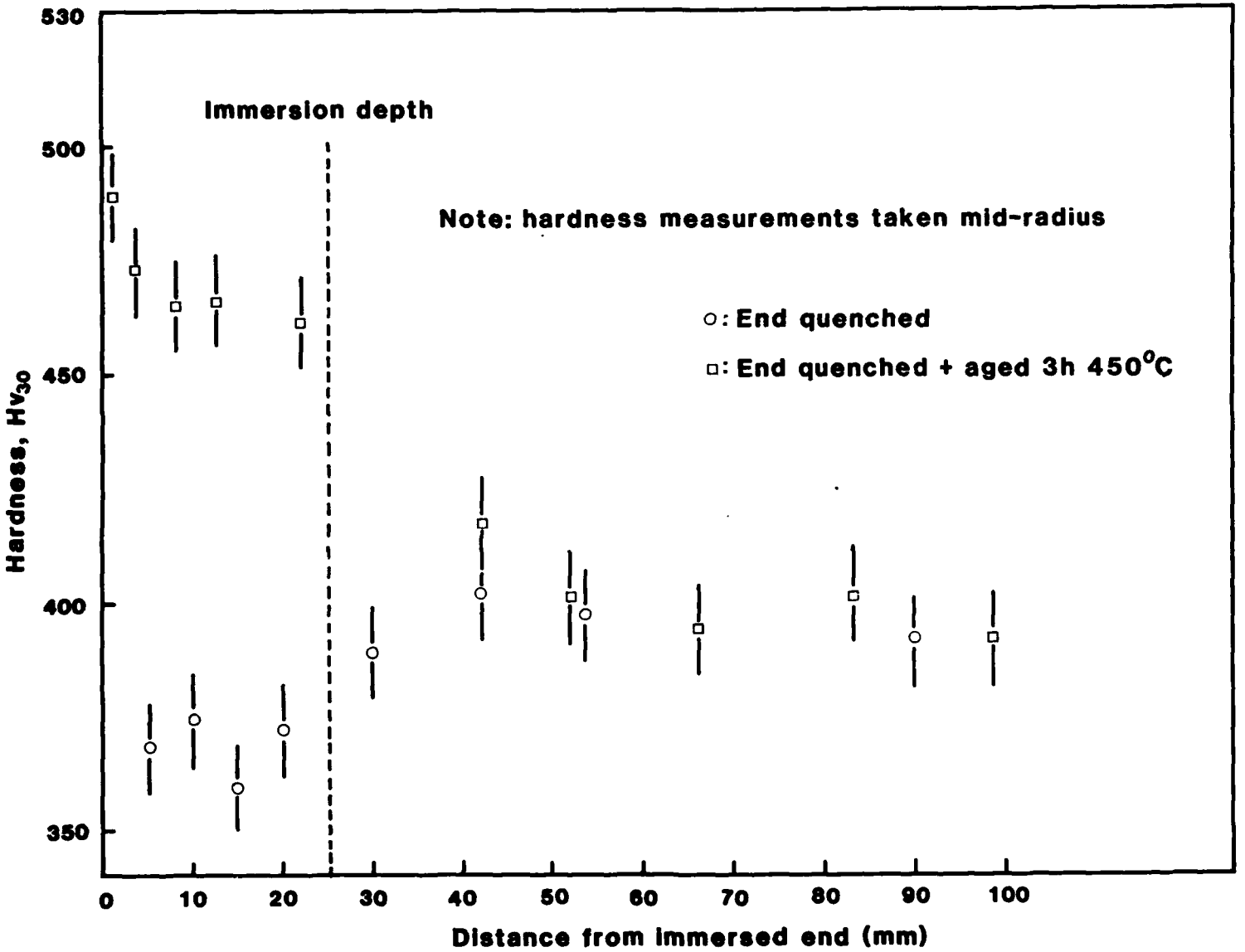

Figure 18 Variation of Vickers hardness with distance in end quenched bars

Figure 19a. *CROSSED POLARS* X 150
F4673

Figure 19b. ETCHED (BRIGHT FIELD) x 150
F4414

Figure 19. Showing microstructure 10mm from end of bar immersed at 100mm/s.

Rol[illegible]

Figure 20. Showing martensitic structure 10mm from end of bar immersed at 100mm/s. ETCHED (BRIGHT FIELD)

x 750
F4415

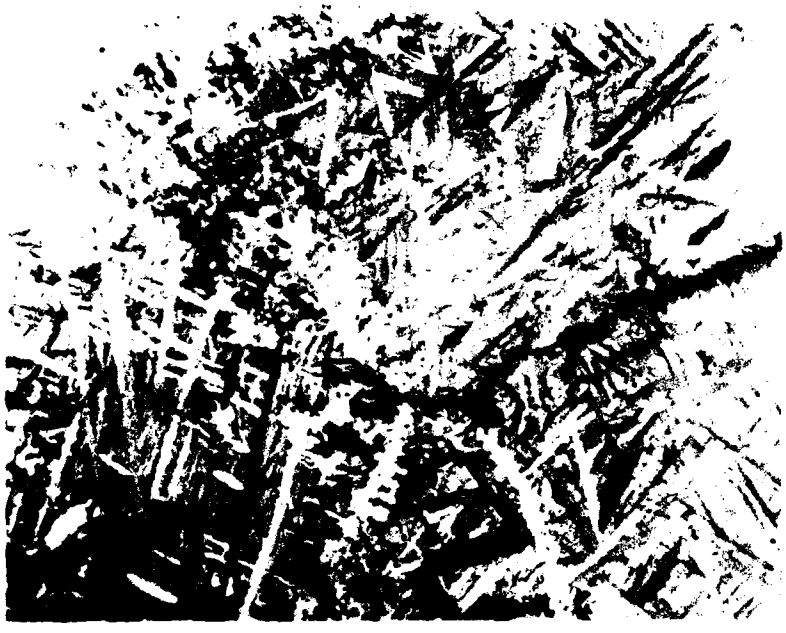

Figure 21. Showing microstructure 35mm from end of bar immersed at 100mm/s.
CROSSED POLARS

x 150
F4674

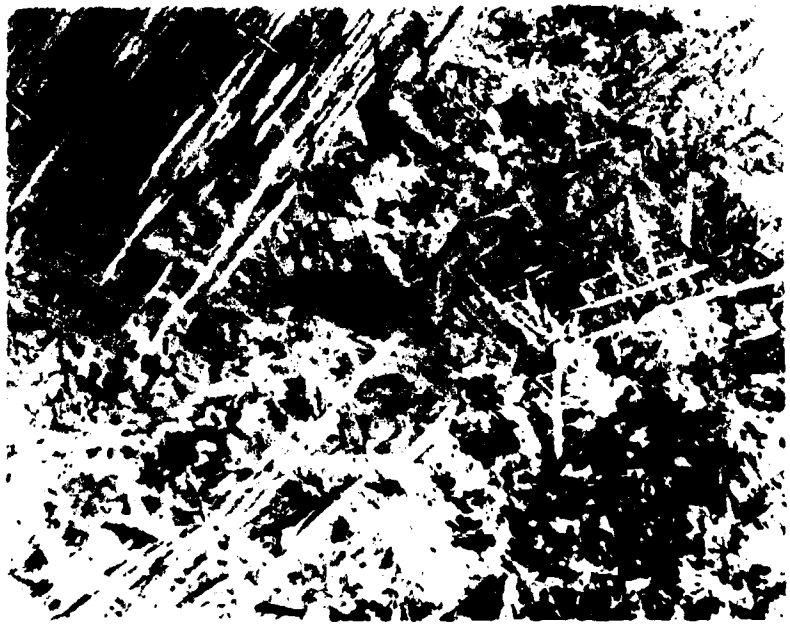

Figure 22. Showing microstructure 50mm from end of bar immersed at 100mm/s.
CROSSED POLARS

x 150
F4410

R812/4

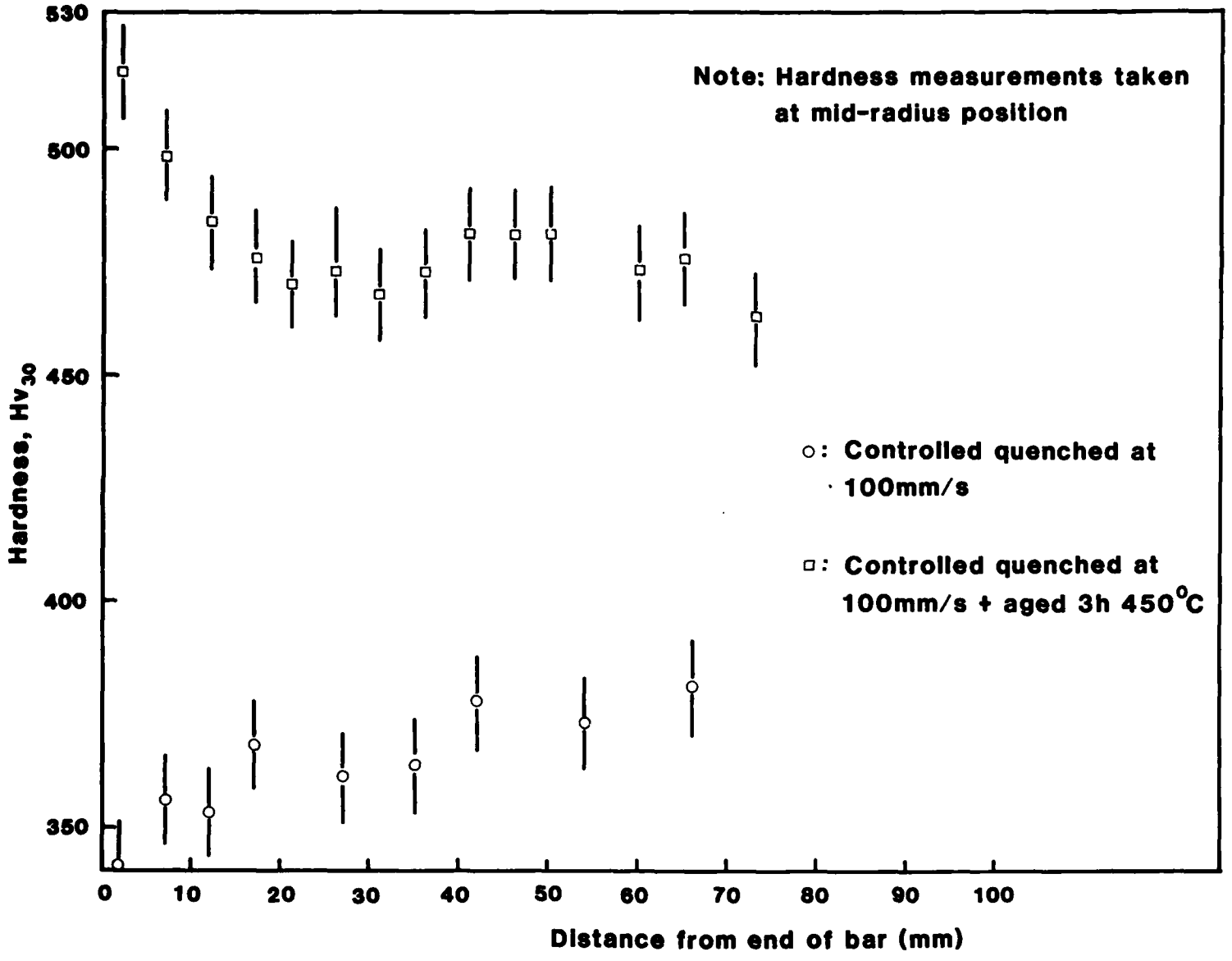

Figure 23 Variation of hardness with distance from end of bar

Figure 24a. *CROSSED POLARS* x 150
F4665

Figure 24b. ETCHED (BRIGHT FIELD) x 150
F4668

Figure 24. Showing microstructure 30mm from end of bar immersed at 10mm/s.

R812/4

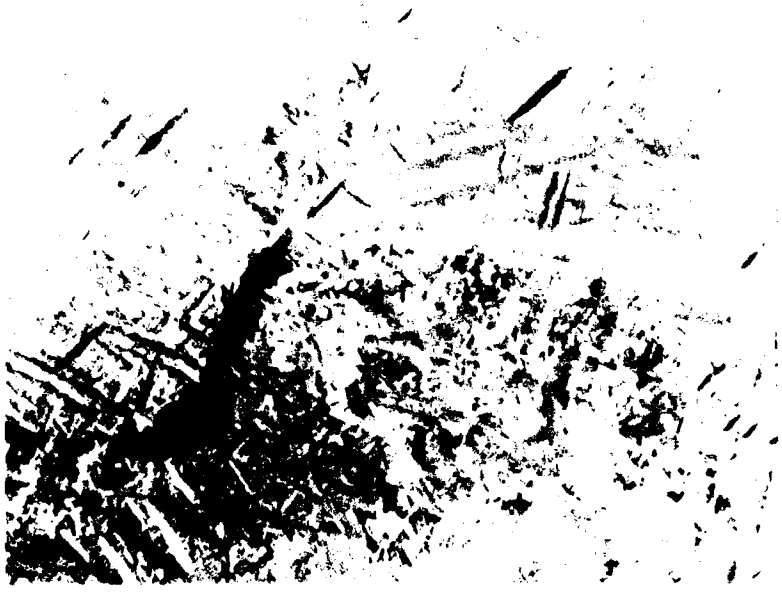

Figure 25. Showing structure 35mm from end of end quenched bar after ageing 3 hours 450°C. x 150
F4670
CROSSED POLARS

Figure 26. Showing structure 70mm from end of end quenched bar after ageing 3 hours 450°C. x 150
F4669
CROSSED POLARS

R812/4

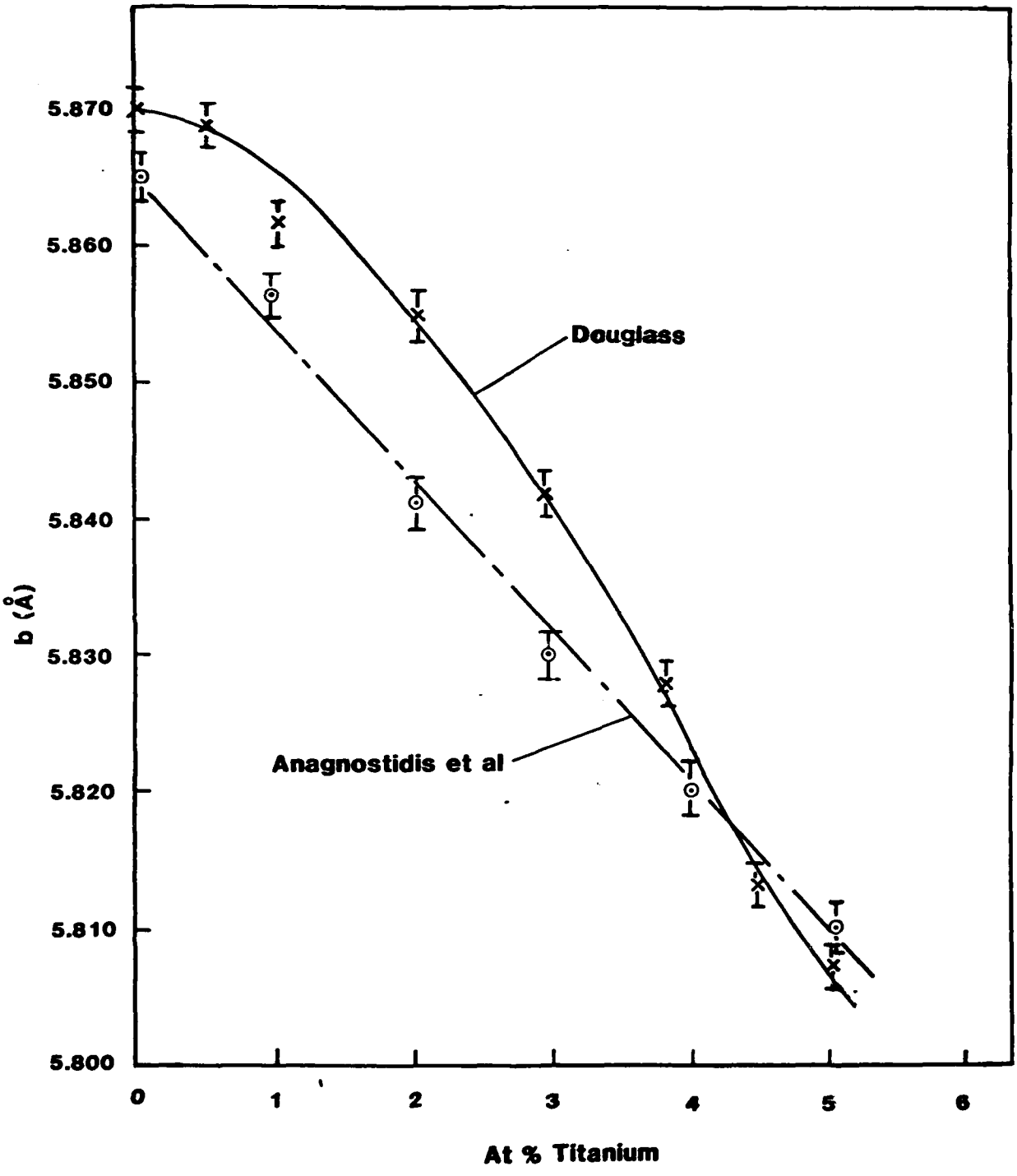

Figure 27 Variation of 'b' lattice parameter with composition according to Anagnostidis et al[13] and Douglass[14]

END

DATE
FILMED
10-81

DTIC